Liquid Crystals
Publication details, including instructions for authors and subscription information:
http://www.informaworld.com/smpp/title~content=t713926090

Thermal behaviour of the thermotropic cubic mesogen 4'-*n*-hexadecyloxy-3'-nitrobiphenyl-4-carboxylic acid (ANBC-16) under hydrostatic pressure

Yoji Maeda; Gui-Ping Cheng; Shoichi Kutsumizu; Shinichi Yano

Online publication date: 06 August 2010

To cite this Article Maeda, Yoji , Cheng, Gui-Ping , Kutsumizu, Shoichi and Yano, Shinichi(2001) 'Thermal behaviour of the thermotropic cubic mesogen 4'-*n*-hexadecyloxy-3'-nitrobiphenyl-4-carboxylic acid (ANBC-16) under hydrostatic pressure', Liquid Crystals, 28: 12, 1785 — 1791
To link to this Article: DOI: 10.1080/02678290110078801
URL: http://dx.doi.org/10.1080/02678290110078801

LIQUID CRYSTALS, 2001, VOL. 28, NO. 12, 1785–1791

Thermal behaviour of the thermotropic cubic mesogen 4′-*n*-hexadecyloxy-3′-nitrobiphenyl-4-carboxylic acid (ANBC-16) under hydrostatic pressure

YOJI MAEDA*, GUI-PING CHENG

Nanotechnology Research Institute,
National Institute of Advanced Industrial Science and Technology, Higashi 1-1,
Tsukuba, Ibaraki 305-8565, Japan

SHOICHI KUTSUMIZU

Instrumental Analysis Center, Gifu University, Yanagido 1-1, Gifu 501-1193, Japan

and SHINICHI YANO

Department of Chemistry, Faculty of Engineering, Gifu University, Yanagido 1-1,
Gifu 501-1193, Japan

(*Received 1 April 2001; accepted 13 June 2001*)

The phase behaviour of 4′-*n*-hexadecyloxy-3′-nitrobiphenyl-4-carboxylic acid (ANBC-16) was investigated under hydrostatic pressures up to 200 MPa using high pressure differential thermal analysis. The phase transition sequence crystal 4 (Cr_4)–crystal 3 (Cr_3)–crystal 2 (Cr_2)–crystal 1 (Cr_1)–smectic C (SmC)–Cubic (Cub)–smectic A (SmA)–'structured liquid' (I_1)–isotropic liquid (I_2) was observed for a virgin sample on heating at atmospheric pressure. The stable temperature region of the optically isotropic cubic phase becomes narrower on increasing pressure and disappears at pressures above 65 MPa. The T vs. P phase diagram exhibits the existence of a triple point (65 MPa, 207.6°C) for the cubic phase, a new mesophase (X), and the SmA phase, indicating the upper limit for the cubic phase. The new mesophase, denoted here as X, appears in place of the cubic phase at pressures above 65 MPa. The phase diagram also indicates that the Cr_4–Cr_3, Cr_3–Cr_2, and Cr_2–Cr_1 transition lines merge at about 40–50 MPa and then only the Cr_4–Cr_1 transition is observed in the solid state at higher pressures. Thus the phase transition process on heating changes from the sequence Cr_4–Cr_3–Cr_2–Cr_1–SmC–Cub–SmA–I_1–I_2 at atmospheric pressure to Cr_4–Cr_1–SmC–X–SmA–I_1–I_2 in the high pressure region above 65 MPa, via Cr_4–Cr_3–Cr_2–Cr_1–SmC–(X)–Cub–SmA–I_1–I_2 in the low pressure region.

1. Introduction

Thermotropic cubic phases have been attracting considerable scientific interest because they are optically isotropic, and their structures and transformations are not fully understood. In 1957, a homologous series of mesomorphic 4′-*n*-alkoxy-3′-nitrobiphenyl-4-carboxylic acids, ANBC-*n*, where *n* is the number of carbon atoms in the alkoxy chain, was synthesized by Gray *et al.* [1]. The polymorphism of the hexadecyloxy ($n = 16$) and octadecyloxy ($n = 18$) derivatives was investigated by Demus *et al.* [2]. This mesophase was initially called the smectic D phase, but is now classified as a cubic phase because the layered smectic structure is inconsistent with its isotropic properties. Since then, increasing attention has focused on its structure and stability [2, 3], and now the ANBC-*n* homologues are known to show cubic phases for *n* in the range 15–26 [4]. The ANBC-*n* molecule consists of a nitrobiphenylcarboxylic acid core and an *n*-alkoxy chain.

Since most of the molecules are dimerized in the solid and liquid crystalline phases via intermolecular hydrogen bonds [5, 6], this system is described as a 'dimerized molecule' which has a long core and two terminal alkoxy

*Author for correspondence; e-mail: yoji.maeda@aist.go.jp

Liquid Crystals ISSN 0267-8292 print/ISSN 1366-5855 online © 2001 Taylor & Francis Ltd
http://www.tandf.co.uk/journals
DOI: 10.1080/02678290110078801

chains. For the cubic phase, two structural models have been proposed. One assumes an ordered packing of spherical micelles [7]; the other is called the interwoven jointed-rod model [8–12]. At present, the latter model is commonly accepted on the basis of experimental results obtained by X-ray diffraction (XRD) [9, 12], NMR spectroscopy [6, 13] and dynamic viscoelastic measurements [14]. For the cubic phase of the hexadecyloxy derivative, Tardieu and Billard [9] have assigned the space group *Ia3d*, and showed that the unit cell volume contains about 1000 molecules. Furthermore, reliable thermodynamic quantities associated with the phase transitions of ANBC-*n* homologues exhibiting cubic phases have been measured by precise calorimetric measurements [15–18].

Recently, Shankar Rao *et al.* investigated the phase behaviour of ANBC-16, by the optical measurement of transmitted light intensity under high pressure [19]. They reported an interesting T vs. P phase diagram for ANBC-16 in which the cubic phase disappeared at 40 MPa, while a columnar (Col) phase appeared between the smectic C (SmC) and smectic A (SmA) phases under high pressure. This interesting pressure effect on the stability of the mesophases prompted us to study the phase behaviour of ANBC-16 under hydrostatic pressure, and in particular to investigate the effect of pressure on the stability of the cubic phase.

One of the authors has studied the phase behaviour of various liquid crystals under hydrostatic pressure using high pressure differential thermal analysis (DTA) and XRD apparatus [20–22]. In this paper, we present the experimental results of the thermal behaviour of ANBC-16 under hydrostatic pressures up to 200 MPa by high pressure DTA measurements. The T vs. P phase diagram constructed here is compared with their phase diagram, in order better to understand the phase behaviour of ANBC-16.

2. Experimental

2.1. *Sample preparation*

ANBC-16 was prepared according to the method described by Gray *et al.* [1]. Samples were recrystallized from ethanol several times and the purity was confirmed by infrared (IR), ^{1}H NMR, mass spectroscopy (MS), and elemental analysis. We used two batches of ANBC-16, samples A and B, which were prepared using essentially the same method. They could not be distinguished on grounds of purity but were purified using slightly different recrystallization procedures.

2.2. *DSC measurements*

ANBC-16 was characterized by differential scanning calorimetry (DSC) and polarizing optical microscopy (POM) under atmospheric pressure. Thermal characterization was performed on a Perkin-Elmer DSC-7 and MacScience DSC 3100S calorimeters at a scanning rate of 5°C min^{-1} under N_2 gas flow. Temperatures and heats of transition were calibrated using the reference materials, indium ($T_m = 156.6$°C, $\Delta H = 28.46$ J g^{-1}) and tin ($T_m = 231.9$°C). The transition temperature was determined as the onset of the transition peak at which the tangential line of the inflection point of the rising part of the peak crosses over the extrapolated baseline. But the temperature of the I_1–I_2 transition was assigned as the peak temperature because of the complexity of the peak, which overlaps peaks associated with the Cub–SmA and SmA–I_1 transitions. The morphological texture of sample B was observed with a Leitz Orthoplan polarizing optical microscope equipped with a Mettler FP-82 hot stage at a heating/cooling rate of 0.5°C min^{-1}.

2.3. *DTA measurements under pressure*

The high pressure DTA apparatus used in this study is described elsewhere [23]. The DTA system was operated in a temperature region between room temperature and 250°C under hydrostatic pressures up to 200 MPa. Dimethylsilicone oil with a medium viscosity (100 cSt) was used as the pressurizing medium. The sample weighing about 4 mg was put in the DTA cell and coated with epoxy adhesives, in order to fix the sample to the bottom of the cell and also to prevent direct contact with the silicone oil. The DTA runs were performed at a constant scan rate of 5°C min^{-1} under various pressures. Transition temperatures were determined in the same manner as in the DSC analysis. As ANBC-16 is not very thermally stable, a virgin sample was used for each DTA heating run.

3. Results and discussion

3.1. *Characterization of ANBC-16 at atmospheric pressure*

Figure 1 shows the DSC heating curve of ANBC-16, specifically a virgin sample of B, at a scanning rate of 5°C min^{-1}. One can see three small peaks in the solid state at 47.5, 74.5 and 89.4°C, a major peak at 124.9°C, a small but sharp peak at 175.1°C, double peaks at 197.9 and 198.8°C, and finally a broad peak at 203.1°C. All of the peaks are endothermic and thermodynamically first order transitions. These peaks are assigned as the Cr_4–Cr_3, Cr_3–Cr_2, and Cr_2–Cr_1 transitions for the first three peaks, the Cr_1–SmC transition for the major peak, the SmC–Cub transition for the sharp peak at 175°C, the Cub–SmA and SmA–I_1 transitions for the double sharp peaks, and finally the I_1–I_2 transition for the broad peak at the highest temperature. The I_1–I_2 transition is the transition from the 'ordered' liquid containing dimerized

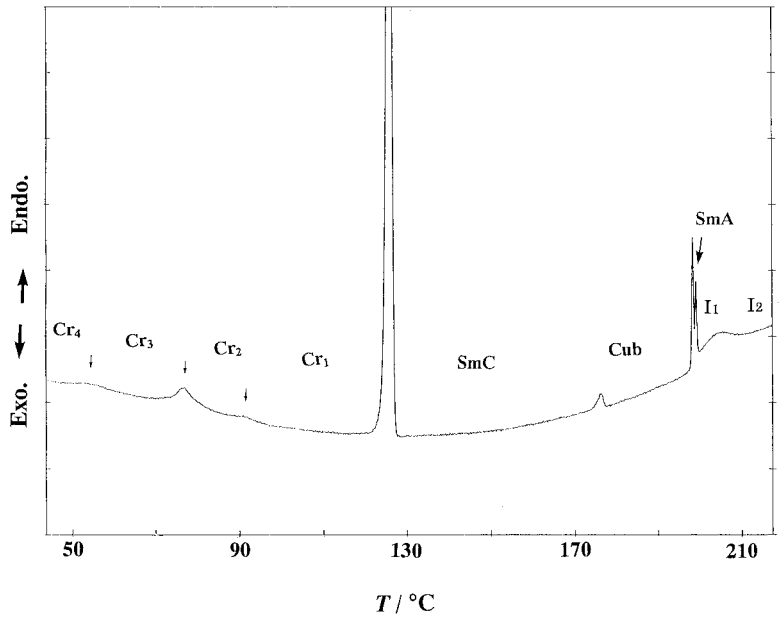

Figure 1. DSC heating curve for a virgin sample of B of ANBC-16: heating rate 5°C min^{-1}

ANBC-16 molecules to the truly isotropic liquid consisting of isolated molecules [4]. The table lists the thermodynamic data associated with these transitions.

Figure 2 shows the POM photographs of ANBC-16 observed on heating at 2°C min^{-1}. One can see in figure 2(*a*) the spherulitic texture of the crystals at 25°C, in (*b*) the fluid-like texture of SmC phase at 150°C, and in (*c*) the texture associated with the SmC–Cub transition at 179°C, in which the black, isotropic areas of the cubic phase have quite distinctive shapes—squares, rectangles, and rhombohedrons. These growing areas eventually coalesce to give an optically isotropic field of view which remains until many small bright portions of the SmA phase appear at about 201°C. Finally the completely black areas of the isotropic liquid phase occur at about 203°C.

3.2. *Thermal behaviour of ANBC-16 under pressure*

Figure 3 shows the DTA heating behaviour in the solid state for the sample A of ANBC-16 at various pressures from 9 to 52 MPa. The DTA heating curves at pressures up to 30 MPa show clearly three small peaks and a major peak, associated with the Cr_4–Cr_3, Cr_3–Cr_2, and Cr_2–Cr_1 transitions, and the Cr_1–SmC transition (melting), respectively, in order of increasing temperature. These DTA traces at low pressures, below 30 MPa, correspond well with the DSC curve shown in figure 1. It is noted here that the first three peaks become closer on increasing the pressure and then merge, apparently into a peak associated with a Cr_4–Cr_1 transition at about 55 MPa, indicating that both the Cr_3 and Cr_2 phases disappear above this pressure. The Cr_4–Cr_1 transition is observed as a single peak with a relatively large transition enthalpy under high pressures.

Figure 4 shows the DTA heating curves of the sample B of ANBC-16 over the whole temperature region but in the same pressure range as figure 3. The DTA curve at 10 MPa contains two small peaks associated with the Cr_4–Cr_3 and Cr_3–Cr_2 transitions, a major peak for the Cr_1–SmC transition, a small but sharp peak for the SmC–Cub transition, and finally the double peaks for the Cub–SmA and SmA–I_1 transitions, in order of increasing temperature. Unfortunately the Cr_2–Cr_1 transition was not seen in this sample. This is in part due to slightly different recrystallization conditions used for the samples, and also due to the low sensitivity of the high pressure DTA apparatus. Except for the Cr_2–Cr_1 transition, all the DTA peaks seen at 10 MPa correspond

Table. Thermodynamic quantities associated with the phase transitions of ANBC-16. Heating rate: 5°C min^{-1}.

T/°C, (ΔH/kJ mol^{-1})							
Cr_4–Cr_3	Cr_3–Cr_2	Cr_2–Cr_1	Cr_1–SmC	SmC–Cub	Cub–SmA	SmA–I_1	I_1–I_2
47.5 (0.5_6)	74.5 (2.3_2)	89.4 (0.1_6)	124.9 (38.5_8)	175.1 (0.5_5)	197.9 (1.5_1)	198.8 (0.9_5)	203.1 (4.0_0)

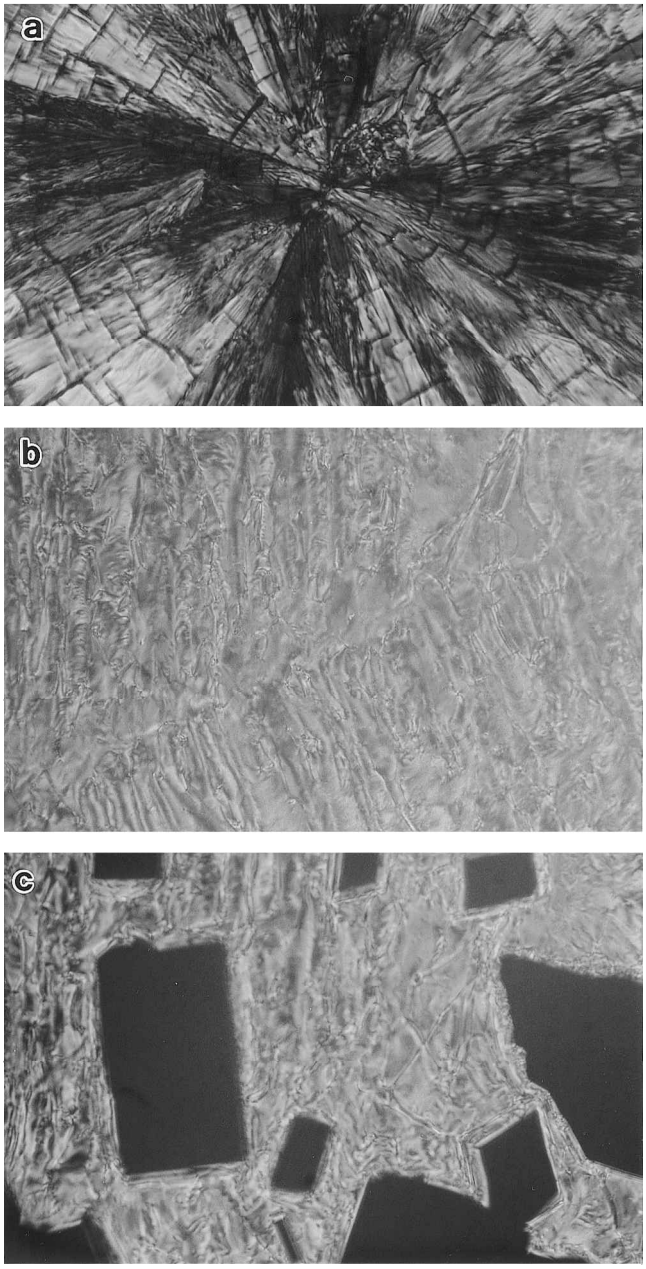

Figure 2. POM photographs of ANBC-16 obtained on heating: (*a*) crystal spherulite at 25°C, (*b*) texture of the SmC phase at 150°C, (*c*) texture of the cubic phase (rectangular black, and thus optically isotropic areas) appearing in the SmC phase at 178°C.

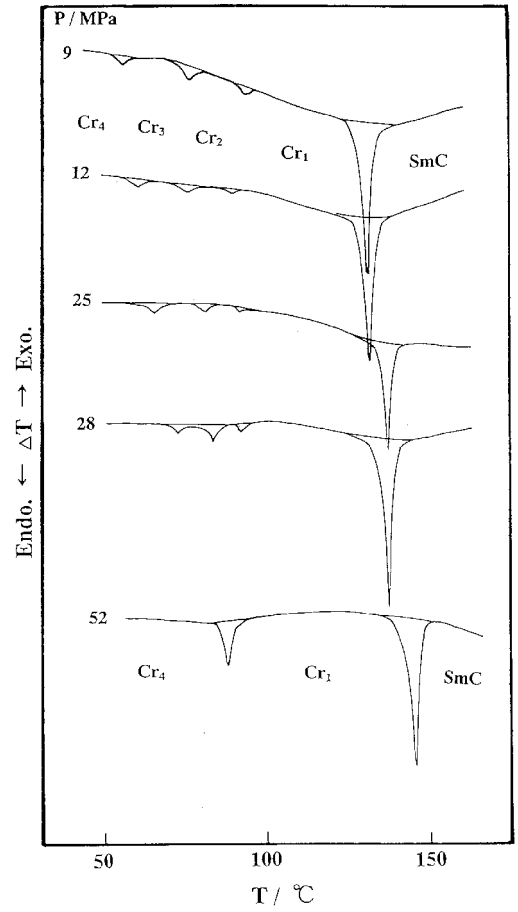

Figure 3. DTA heating curves in the solid-state temperature range for a virgin sample of A of ANBC-16 at various pressures from 9 to 52 MPa: heating rate 5°C min^{-1}.

well with those of the DSC curve shown in figure 1. At higher temperatures than the major peak associated with the Cr_1–SmC transition, a small peak for the SmC–Cub transition was observed at 178°C. Then the combined peaks associated with the Cub–SmA and SmA–I_1 transitions were observed at 198 and 202°C, respectively. In addition, the I_1–I_2 transition peak was often observed as a high temperature shoulder on the SmA–I_1 transition.

As illustrated in figure 4, the two peaks associated with the Cr_4–Cr_3 and Cr_3–Cr_2 transitions also become closer with increasing pressure (see at 32 and 35 MPa), and then the peaks merge to a single peak associated with the Cr_4–Cr_1 transition at about 57 MPa; this is similar to the behaviour seen in figure 3. It is found that the stable temperature region of the cubic phase decreases on increasing the pressure and disappears at high pressures above about 65 MPa.

Figure 5 shows the DTA heating curves of the sample B in the high pressure range between 90 and 160 MPa. The cubic phase is lost in this pressure region, while a new peak appears at a temperature between the major peak and where the SmC–Cub transition was. This indicates that a new mesophase appears in place of the cubic phase between the SmC and SmA phases under higher pressures. The mesophase is tentatively named here as X phase. The transition sequence in the pressure range above about 65 MPa is expressed as Cr_4–Cr_1–SmC–X–SmA–I_1–I_2.

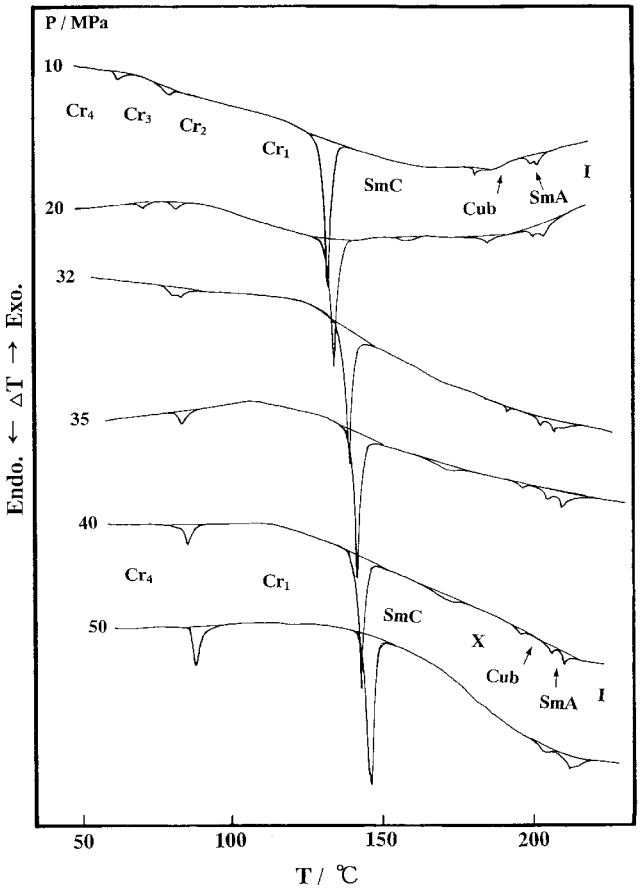

Figure 4. DTA heating curves for a virgin sample of B of ANBC-16 at various pressures from 10 to 50 MPa: heating rate 5°C min^{-1}.

Figure 6 shows the T vs. P phase diagram of ANBC-16 in the pressure range up to 200 MPa. The transition curves can be expressed approximately as first order polynomials in terms of pressure as follows:

$0.1 < P <$ *c.* 65 MPa	
Cr_4–Cr_3 transition	$T = 47.2 + 0.697_2\ P$
Cr_3–Cr_2	$T = 77.3 + 0.117_0\ P$
Cr_2–Cr_1	$T = 92.7 - 0.127_0\ P$
SmC–Cub	$T = 173.5 + 0.524_9\ P$
Cub–SmA	$T = 196.9 + 0.165_0\ P$
c. 65 MPa $< P$	
Cr_4–Cr_1	$T = 77.1 + 0.195_2\ P$
SmC–X	$T = 172.8 + 0.177_2\ P$
X–SmA	$T = 192.2 + 0.226_9\ P$
Whole pressure range	
Cr_1–SmC	$T = 127.4 + 0.294_0\ P$
SmA–I_1	$T = 199.4 + 0.222_4\ P$
I_1–I_2	$T = 203.9 + 0.242_5\ P$.

The transition points estimated by these equations are in relatively good agreement with the corresponding DSC data, except for a relatively large difference of ± 3°C in the crystal–crystal transitions. This is mainly due to the low precision of the high pressure DTA apparatus. If this is taken into account, these equations seem to be good approximations for the T vs. P relationships for each phase transition of ANBC-16 in the observed pressure range.

Several interesting features are evident in the T vs. P phase diagram of ANBC-16. Firstly, the stable temperature region of the cubic phase decreases with increasing

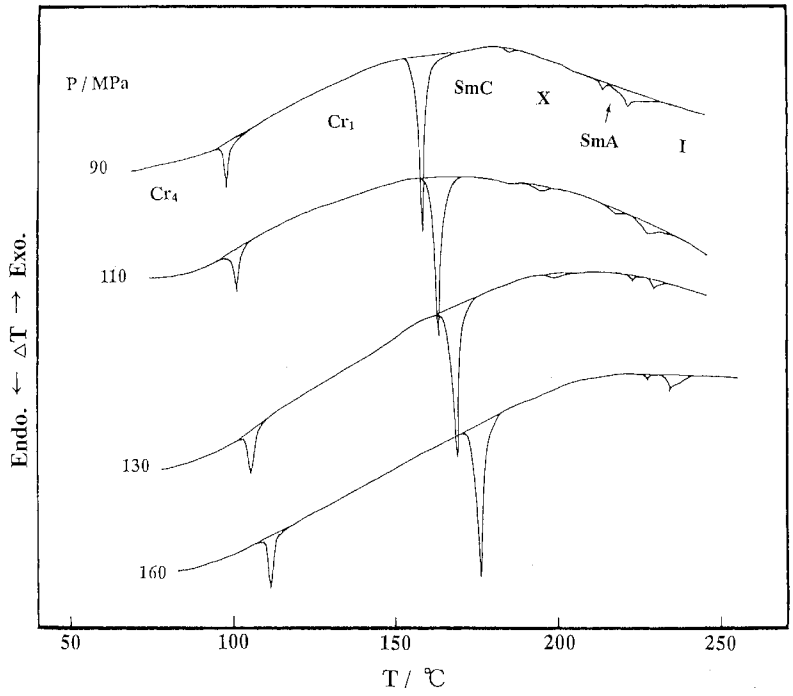

Figure 5. DTA heating curves for a sample of B of ANBC-16 at various high pressures: heating rate 5°C min^{-1}.

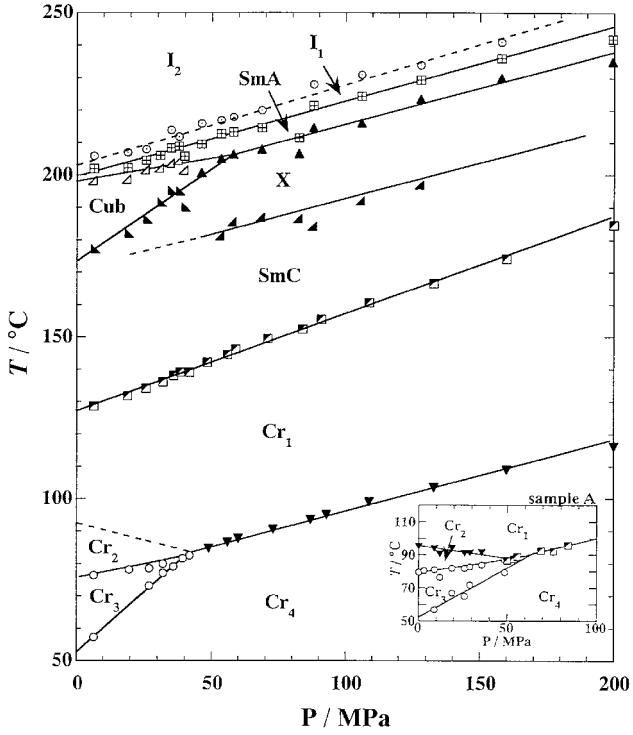

Figure 6. *P* vs. *T* phase diagram of the sample B of ANBC-16. The inset shows the Cr_4–Cr_3, Cr_3–Cr_2, and Cr_2–Cr_1 transition lines of sample A.

pressure as shown in figure 6, and the cubic phase disappears at about 65 MPa. The triple point for the cubic, X, and SmA phases, indicating the upper limit for the cubic phase, is estimated to be 65 MPa and 207.6°C by extrapolation of the above equations for the SmC–Cub and Cub–SmA transitions. Shankar Rao *et al.* [19] reported a *T* vs. *P* diagram for ANBC-16 in which the cubic phase disappeared at 40 MPa, while a columnar (Col) phase appeared between the SmC and SmA phases under high pressures. In general a similar trend is observed in this study, but one can see a large difference in the triple point: their triple point (about 40.5 MPa and 188°C) is for the SmC, Cub, and Col phases, while the triple point in this case is for the Cub, SmA and X phases. They stated that the Cub–Col transition line has a negative slope (dT/dP) with pressure and that the cubic phase transforms into the SmA phase via the Col phase in the low pressure range. The *T* vs. *P* diagram in this study, however, exhibits no transition lines with a negative slope, except for the Cr_2–Cr_1 transition. The cubic phase grows from the SmC phase, probably via the X phase in the low pressure range below 50 MPa, and then transforms directly into the SmA phase. This is an important difference between the two *T* vs. *P* diagrams.

Secondly, a new mesophase (X) appears between the SmC and SmA phases at pressures above about 65 MPa, replacing the cubic phase. When the SmC–X transition line is extrapolated linearly to low pressures, see figure 6, the transition becomes close to the SmC–Cub transition in the neighbourhood of atmospheric pressure. Thus, one can expect that the X phase would appear between the SmC and cubic phases in the low pressure region, although the X phase was not clearly observed.

Thirdly, it is noted that both the SmA and I_1 phases are stable even at the highest pressures studied since the X–SmA and SmA–I_1 transitions are observed in the high pressure region. Furthermore, the I_1–I_2 transition was often observed as a high temperature shoulder to the SmA–I_1 transition peak. Shankar Rao *et al.* [19] did not comment further on the I_1–I_2 transition, but the phenomenon indicates clearly the pressure independence of the 'ordered liquid' (I_1)–isotropic liquid (I_2) transition of the dimerized ANBC-16 molecules.

Fourthly, it is noted that the Cr_3 and Cr_2 phases disappear at high pressures above about 40–55 MPa. It is found that these crystal–crystal transitions of ANBC-16 merge into the Cr_4–Cr_1 transition under higher pressures. This behaviour of the crystal–crystal transitions is very interesting because the phenomenon seems to be related to the disappearance of the cubic phase under high pressure. The Cr_4–Cr_1 transition has a relatively large enthalpy change and is observed in the solid state under pressures above 65 MPa, and the Cr_4 and Cr_1 phases are stable as the low and high temperature crystal forms, respectively.

It should be emphasized that the cubic phase is destabilized with increasing pressure and finally disappears at high pressures above 65 MPa. This supports experimentally a qualitative interpretation that thermal fluctuations and destabilization of the SmC layered structure, which is effectively reduced by hydrostatic pressure, results in a curved interfacial structure such as the cubic structure [24]. However, the appearance of the X phase between the SmC and SmA phases is an unexpected result that is hopefully a key to understanding the transformation from the SmC to the cubic structures. Recently, it was found that ANBC-22 and ANBC-26 show two types of cubic phases, one with *Ia3d* symmetry and the other with *Im3m* symmetry [25, 26], reflecting that their stabilities are very sensitive to temperature and alkoxy chain length *n*. Thus there is a possibility of X being either another cubic modification as shown in ANBC-22 and ANBC-26 or a different smectic modification from the SmC and SmA phases. Structural identification of the X phase should now be performed under pressure.

We thank Mr Koushi Morita and Mr Tatsuya Ichikawa of Gifu University for their experimental assistance.

References

[1] Gray, G. W., Jones, B., and Marson, F., 1957, *J. chem. Soc*., 393.

[2] Demus, D., Kunicke, G., Neelsen, J., and Sackmann, H., 1968, *Z. Naturforsch*., **23a,** 84.

[3] Gray, G. W., and Goodby, J. W., 1984, *Smectic Liquid Crystals—Textures and Structures* (Glasgow: Leonard Hill), Chap. 4.

[4] Kutsumizu, S., Yamada, M., and Yano, S., 1994, *Liq. Cryst*., **16,** 1109.

[5] Kutsumizu, S., Kato, R., Yamada, M., and Yano, S., 1998, *J. phys. Chem. B*, **101,** 1666.

[6] Tansho, M., Onoda, Y., Kato, R., Kutsumizu, S., and Yano, S., 1998, *Liq. Cryst*., **24,** 525.

[7] Diele, S., Brand, P., and Sackmann, H., 1972, *Mol. Cryst. liq. Cryst*., **17,** 163.

[8] Luzzati, V., and Spegt, A., 1967, *Nature*, **215,** 701.

[9] Tardieu, A., and Billard, J., 1976, *J. Phys. (Paris) Coll*., **37,** C3-79.

[10] Etherington, G., Leadbetter, A. J., Wang, X. J., Gray, G. W., and Tajbakhsh, A., 1986, *Liq. Cryst*., **1,** 209.

[11] Levelut, A.-M., and Fang, Y., 1991, *Colloq. Phys*., **23,** C7-229.

[12] Levelut, A.-M., and Clerc, M., 1998, *Liq. Cryst*., **24,** 105.

[13] Ukleja, P., Siatkowski, R. E., and Neubert, M., 1988, *Phys. Rev. A*, **38,** 4815.

[14] Yamaguchi, T., Yamada, M., Kutsumizu, S., and Yano, S., 1995, *Chem. Phys. Lett*., **240,** 105.

[15] Saito, K., Sato, A., and Sorai, M., 1998, *Liq. Cryst*., **25,** 525.

[16] Morimoto, N., Saito, K., Morita, Y., Nakasuji, K., and Sorai, M., 1999, *Liq. Cryst*., **26,** 219.

[17] Sato, A., Saito, K., and Sorai, M., 1999, *Liq. Cryst*., **26,** 341.

[18] Sato, A., Yamamura, Y., Saito, K., and Sorai, M., 1999, *Liq. Cryst*., **26,** 1185.

[19] Shankar Rao, D. S., Krishna Prasad, S., Prasad, V., and Kumar, S., 1999, *Phys. Rev. E*, **59,** 5572.

[20] Maeda, Y., Yun, Y.-K., and Jin, J.-I., 1998, *Thermochim. Acta*, **322,** 101.

[21] Maeda, Y., and Shimizu, Y., 1999, *Liq. Cryst*., **26,** 787; Maeda, Y., and Shimizu, Y., 1999, *Liq. Cryst*., **26,** 1067.

[22] Maeda, Y., Osada, K., and Watanabe, J., 2000, *Macromolecules*, **33,** 2456.

[23] Maeda, Y., and Kanetsuna, H., 1985, *Bull. Res. Inst. Polym. Tex*., **149,** 119; Maeda, Y., 1990, *Thermochim. Acta*., **163,** 211.

[24] Charvolin, J., and Sadoc, J.-F., 1988, *J. phys. Chem*., **92,** 5787.

[25] Kutsumizu, S., Ichikawa, T., Nojima, S., and Yano, S., 1999, *Chem. Commun*., 1181.

[26] Kutsumizu, S., Ichikawa, T., Yamada, M., Nojima, S., and Yano, S., 2000, *J. phys. Chem. B*, **104,** 10196.